



Quantitative analysis of contrast-enhanced ultrasonography in rat models of hepatic acute graft-versus-host disease

Yuwei Xin^{1#^}, Yu Xiong^{1#^}, Feifei Liu^{1,2^}, Linlin Qu^{3^}, Wenxue Li^{1^}, Li Yang^{1^}, Yiqun Liu^{1^}, Jia'an Zhu^{1^}

¹Department of Ultrasound, Peking University People's Hospital, Beijing, China; ²Department of Ultrasound, Binzhou Medical University Hospital, Binzhou, China; ³Department of Pathology, Peking University People's Hospital, Beijing, China

Contributions: (I) Conception and design: Y Xin, Y Xiong, J Zhu, Y Liu; (II) Administrative support: J Zhu, Y Liu; (III) Provision of study materials or patients: Y Xin, Y Xiong; (IV) Collection and assembly of data: Y Xin, Y Xiong, F Liu, L Qu, W Li, L Yang; (V) Data analysis and interpretation: Y Xin, Y Xiong, F Liu, Y Liu, J Zhu; (VI) Manuscript writing: All authors; (VII) Final approval of manuscript: All authors.

[#]These authors contributed equally to this work.

Correspondence to: Jia'an Zhu, PhD; Yiqun Liu, MD; Department of Ultrasound, Peking University People's Hospital, No. 11 Xizhimen South Street, Beijing 100044, China. Email: zhujaan@pkuph.edu.cn; liuyiqunqun1990@163.com.

Background: Hepatic acute graft-versus-host disease (aGVHD) is a major life-threatening complication of allogeneic hematopoietic stem cell transplantation (allo-HSCT). We hypothesized that contrast-enhanced ultrasound (CEUS) could serve as a new imaging biomarker in early diagnosis of hepatic aGVHD by detecting liver microcirculation.

Methods: Thirty Wistar rats received allo-HSCT were finally included after excluding 9 rats, and they were randomly divided into 5 groups (1- to 5-week groups, 6 per group). Six rats were used for the control group without any intervention. We observed the clinical scores, serum liver enzyme levels and liver CEUS parameters of rats in each group. Hepatic aGVHD was finally confirmed by histopathologic analysis. The diagnostic performance of CEUS parameters in detecting GVHD was evaluated by comparing the area under the receiver operating curve (AUC) values.

Results: After HSCT, the rats developed ruffling of fur, maculopapular rash, weight loss, accompanied by increased clinical scores. Serum liver enzymes were significantly higher than those in the control group from the third week, especially alkaline phosphatase, while CEUS parameters, peak intensity (PI) and mean transit time (MTT), changed in the second week ($P < 0.001$). Compared with non-aGVHD group, the PI was significantly decreased while time to peak and MTT were prolonged in aGVHD group. CEUS parameters were more strongly correlated with pathological grade than serology. PI was an independent predictor for hepatic aGVHD. The AUC of CEUS parameters for diagnosing hepatic aGVHD was 0.933 (95% CI: 0.779–0.992), which was higher than that of clinical scores (AUC = 0.748, 95% CI: 0.557–0.888, $P = 0.032$) and serological markers (AUC = 0.902, 95% CI: 0.737–0.980, $P = 0.694$).

Conclusions: CEUS exhibits promising applications as a quantitative method to detect hepatic aGVHD and early liver damage.

Keywords: Hematopoietic stem cell transplantation (HSCT); hepatic acute graft-versus-host disease (aGVHD); contrast-enhanced ultrasound (CEUS)

[^] ORCID: Yuwei Xin, 0000-0002-2209-7718; Yu Xiong, 0000-0002-7499-7785; Feifei Liu, 0000-0003-2948-4320; Linlin Qu, 0000-0003-1090-2924; Wenxue Li, 0000-0001-7237-7788; Li Yang, 0000-0003-3254-9789; Yiqun Liu, 0000-0001-8417-2915; Jia'an Zhu, 0000-0001-8700-639X.

Submitted Oct 19, 2022. Accepted for publication May 09, 2023. Published online May 22, 2023.

doi: 10.21037/qims-22-1145

View this article at: <https://dx.doi.org/10.21037/qims-22-1145>

Introduction

Allogeneic hematopoietic stem cell transplantation (allo-HSCT) is a well-established treatment for many refractory hematologic malignancies. Unfortunately, graft-versus-host disease (GVHD) is the most common fatal complication of HSCT. It is a major cause of post-transplantation morbidity and mortality, especially higher-grade acute GVHD (aGVHD) (1), which largely restricts its clinical use. Acute GVHD occurs when donor immune cells attack vulnerable host tissues, especially the skin, gastrointestinal tract, and liver (2,3). 30% to 50% of patients reportedly experience aGVHD, with a cumulative incidence of 6.7% in the liver (4,5). Current evidence suggests that hepatic GVHD is an independent risk factor for higher non-relapse mortality, poor relapse-free survival, and overall survival (6). The long-term survival rate of aGVHD ranges from 5% to 80%, depending on disease grade and preventive and therapeutic interventions adopted (1,2,7). Accordingly, the early diagnosis of aGVHD and timely implementation of immunosuppressant agents are essential to improve patient prognosis.

The diagnosis of acute hepatic GVHD primarily relies on clinical and laboratory findings (8), but it lacks specificity and overlaps with other drug toxicities and infectious liver diseases. Therefore, the histopathological assessment provides an important basis. However, biopsy has several limitations, including some of the complications (post-biopsy hemorrhage, and biopsy-related infections) associated with invasiveness and false-negative results (9,10), especially the need for biopsy in patients with immunosuppressive therapy which is still debated (11). In addition, the biopsy is limited by sampling and cannot assess the overall liver involvement and thus delay diagnosis, resulting in GVHD progression to grades 3–4 and poor patient outcomes. These findings emphasize the need to develop an effective non-invasive imaging technique for the early diagnosis and surveillance of aGVHD in the liver. Studies have shown that hepatic aGVHD exhibits non-specific imaging features, including enhancement of the biliary tract, gallbladder wall thickening, dilatation of the common bile duct, pericholecystic fluid, and biliary sludge (7), making it difficult to distinguish it from other common liver diseases.

Contrast-enhanced ultrasound (CEUS) is also a promising technology for noninvasive imaging with no risk of ionizing radiation or nephrotoxicity, allowing safe administration more than once. It allows a dynamic coverage of the hepatic microcirculation during real-time ultrasonography imaging to achieve visualization of the microvasculature from early arterial until late parenchymal period. Software analysis of CEUS can quantitatively evaluate blood flow and perfusion in the region of interest (ROI) of the liver using the time-intensity curve (TIC). Therefore, CEUS has been widely applied in microcirculation assessment and monitoring treatment response of liver cancer (12) and liver fibrosis (13). However, there are few studies on the application of CEUS in hepatic aGVHD, even though it has been shown that CEUS can be an effective tool to assess and monitor the progression of intestinal GVHD (14,15).

In this study, we aimed to explore the diagnostic value of CEUS for hepatic aGVHD by analyzing the quantitative parameters of CEUS, especially in the early stages. Moreover, we investigated the correlation between CEUS parameters, clinical scores, serological results, and pathological grades and compared their diagnostic efficacy for hepatic aGVHD. We present this article in accordance with the ARRIVE reporting checklist (available at <https://qims.amegroups.com/article/view/10.21037/qims-22-1145/rc>).

Methods

Animal model of aGVHD

The study was approved by the Animal Care and Use Committee of Peking University People's Hospital (License number: 2020PHE088). All experimental procedures were performed according to the Guide for the Care and Use of Laboratory Animals. Forty-five female Wistar rats (Beijing Vital River Laboratory Animal Technologies Co. Ltd, China) aged 6–8 weeks and weighing 180–220 g, and 10 male Fischer 344 rats (Beijing Vital River Laboratory Animal Technologies Co. Ltd, China) were used in this study. All rats were in good health. They were allowed to acclimate to a specific pathogen-free (SPF) experimental environment for 7 days before initiation of the experiment.

They were maintained in separate cages under 12 h light/dark cycles with free access to food and water. All Wistar rats were numbered by another researcher and the standard =RAND() function in Microsoft Excel was used as a random method. We randomly selected 6 normal Wistar rats as the control group (n=6) and the other 39 Wistar rats as recipients that underwent bone marrow transplantation. Ten Fischer 344 rats were used as donors.

We established the aGVHD rat model as previously described (16). Donor Fischer 344 rats were euthanized using CO₂ inhalation. Bone marrow (BM) cells were harvested by flushing their femur and tibia bone marrow with cold RPMI 1640. After red blood cells were removed with Tris-NH₄Cl, the BM cells were centrifuged at 1,000 rpm for 5 minutes and filtered with a nylon filter screen. The spleens were extracted from Fischer 344 rats, minced and ground into single cells. The spleen lymphocytes (SLs) were suspended with RPMI 1640 after the red blood cells were removed with Tris-NH₄Cl. Trypan blue exclusion test detected the viability of BM cells and SLs above 95%. All cells suspension were prepared freshly and used within several hours. Recipient Wistar rats were given myeloablative conditioning with 8 Gy of total-body irradiation prior to injection of a mixture of 4×10⁷ BM cells and 4×10⁷ SLs via the tail vein.

After allo-HSCT, we randomly selected 6 rats at fixed time points every week for observation until the 5th week after modeling (1- to 5-week groups, n=6/group) (17,18). Accordingly, 30 Wistar rats were included in the final analysis. Nine rats were excluded from this study due to death from infection associated with immunosuppression after transplantation or death from an unknown cause.

Clinical evaluation of aGVHD

At each observed time point after modeling, we assessed the overall condition of transplanted rats by the clinical characteristics scoring system (19), which included weight loss, posture (hunching), activity, fur texture, and skin integrity. The grading criteria for each characteristic are as follows: weight loss (0: <10%; 1: 10–25%; 2: >25%), posture (0: normal; 1: hunched back only at rest; 2: severe hunched back impairs movement), activity (0: normal; 1: mild to moderately activity decreased; 2: active only at the time of the stimulus), fur texture (0: normal; 1: mild to moderate ruffling; 2: severe ruffling), skin integrity (0: normal; 1: scaling of paws/tail; 2: obvious denuded skin). The final clinical score for each rat was recorded as the sum of the

five characteristics scores.

CEUS imaging and TIC analysis

CEUS was performed using Aplio800 Ultrasound System (Canon Medical Systems, Toshiba, Japan) with a linear-array transducer (18 MHz). All ultrasounds were performed by a radiologist with more than 10 years of experience in abdominal ultrasonography and CEUS blinded to the clinical and laboratory results. Identical imaging parameters were set for all rats, including a gain of 75, depth of about 2.0 cm, mechanical index of 0.06, a focus of 92%, a dynamic range of 60 dB and a frame rate of 10 frames per second, according to instructions recommended by current guidelines (20). Before the examination, all rats were fasted for more than 6 h and then anesthetized by intraperitoneal administration of ketamine (60 mg/mL) and xylazine (7.5 mg/mL) (21). The rat was placed in a supine position, and the abdomen was shaved to allow clear ultrasound imaging of the liver. We used SonoVue (Bracco, Milan, Italy), a second-generation ultrasound contrast agent widely used clinically, mainly composed of 2.5-µm-diameter microbubbles. When the abdominal aorta, portal vein, and inferior vena cava were observed in transverse-section in the gray-scale ultrasound, we switched to the CEUS mode. Subsequently, the contrast procedure was initiated while bolus injection of 0.2 mL contrast agent via the tail vein, then flushed with 1 mL physiologic saline. Digital cine loops of the entire 180 s CEUS procedure were stored in DICOM format, including the arterial, portal venous, and late phase, for subsequent analysis.

DICOM images were analyzed with the data processing software from the ultrasound instrument and generated a TIC of the ROI. After liver parenchyma enhancement with 10–15 s of image acquisition, we placed 3 circular ROIs with a diameter of 2 mm in the right lobe avoiding large blood vessels and created TICs (*Figure 1*). The following parameters of CEUS were assessed according to TICs: the peak intensity (PI), which is the maximum intensity of the contrast agent in the liver parenchyma; the time to peak (TTP), which is the time required for the liver to exhibit maximum contrast intensity and the mean transit time (MTT), which is the time required for the liver to exhibit half peak wash-out intensity. The mean values of these parameters were used for further analysis. The CEUS images were analyzed separately by the operating radiologist and another equally experienced radiologist to further determine interobserver agreement.

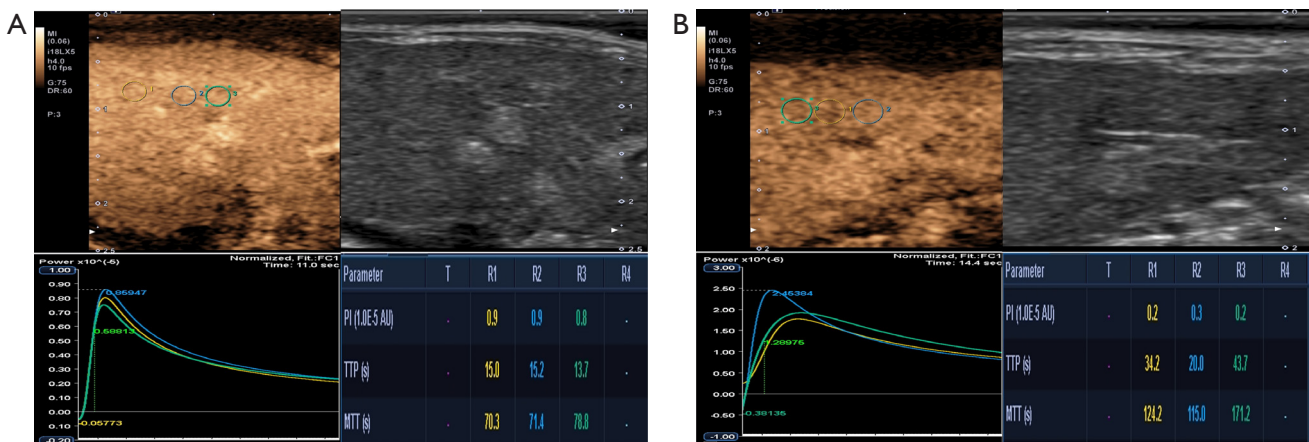


Figure 1 Quantitative analysis of CEUS in the liver of rats with non-acute GVHD and acute GVHD confirmed by histological. B-scan and the CEUS mode display in parallel. TIC and quantitative parameters were simultaneously generated after placing the ROIs in the liver parenchyma. (A) Quantitative analysis of CEUS in non-acute GVHD group. (B) Quantitative analysis of CEUS in acute GVHD group. CEUS, contrast-enhanced ultrasonography; GVHD, graft-versus-host disease; TIC, time intensity curve; ROI, region of interest.

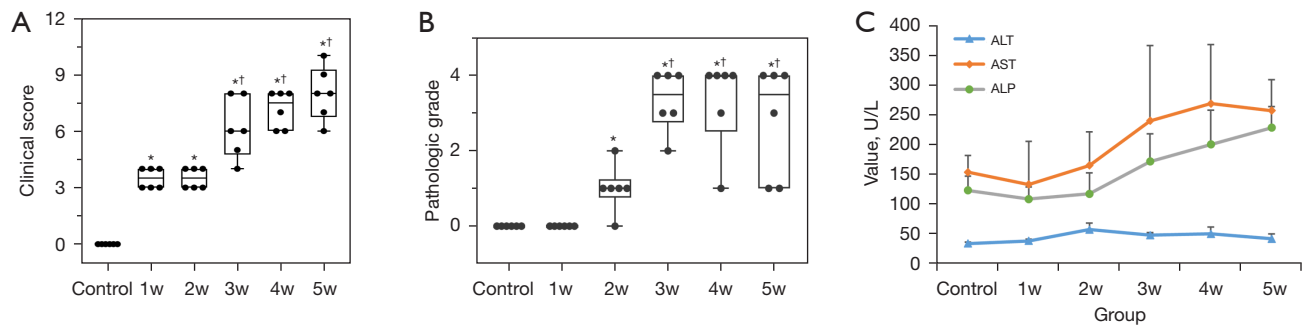


Figure 2 Clinical scores, pathological grades, and serological results (ALT, AST, ALP values) of normal and hepatic acute GVHD rats at various time points after HSCT (6 rats per group). (A) The distributions of clinical scores in each group. *, $P < 0.05$ versus the control group; †, $P < 0.05$ versus the 1w and 2w group. (B) The distributions of pathological grades in each group. *, $P < 0.05$ versus the control and 1w groups; †, $P < 0.05$ versus the 2w group. (C) The line chart of serum ALT, AST, and ALP level at various time points. w, week; GVHD, graft-versus-host disease; HSCT, hematopoietic stem cell transplantation; ALT, alanine aminotransferase; AST, aspartate aminotransferase; ALP, alkaline phosphatase.

Serological test

After contrast-enhanced ultrasonography at the indicated time points (normal group, 1- to 5-week groups after modeling) (Figure 2), 2 mL blood was drawn from the medial canthus vein of each rat, and the serum was separated and stored at -80°C for later use. The level of serum alanine aminotransferase (ALT), aspartate aminotransferase (AST) and alkaline phosphatase (ALP) clinically used to evaluate hepatic aGVHD was detected by a Mindray® automated hematology analyzer (BS-350E, Shenzhen Mindray Bio-Medical Electronics Co., Ltd, Shenzhen, China).

Histopathologic analysis

The rats were euthanized after CEUS and blood sample collection using CO_2 inhalation, according to the euthanasia guidelines of the American Veterinary Medical Association. The excised right liver lobe tissue samples were fixed in 10% formalin, embedded in paraffin, cut into 3 μm thick sections and conducted Hematoxylin and eosin (HE) staining according to standard protocols. Histopathological alterations in the liver parenchyma were assessed by a pathologist with 10 years of experience. Hepatic aGVHD pathology was scored on the 5-grade

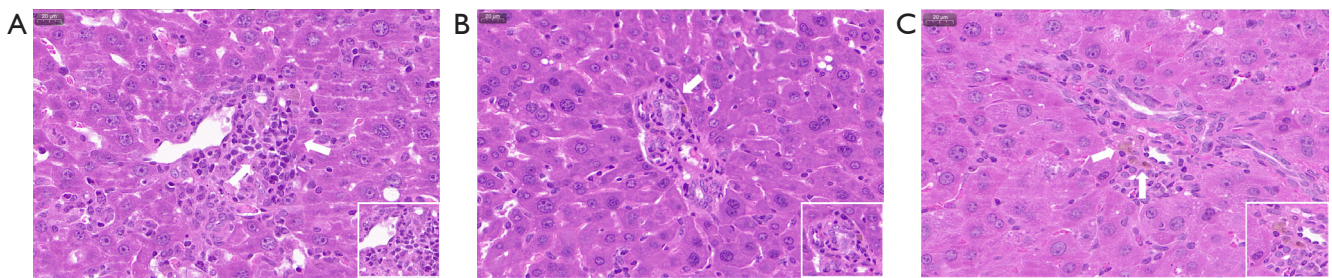


Figure 3 Histological findings of liver in hepatic acute GVHD rats by hematoxylin and eosin staining. The liver histopathological changes in acute GVHD rats included (A) lymphocytic infiltration of the portal areas (arrows), (B) loss of bile duct cells (arrows) and (C) cholestasis (arrows) (original magnifications: $\times 400$; scale bar 20 μm). GVHD, graft-versus-host disease.

scale (22): grade 0 (none); grade 1 (slight inflammation of portal triads or lobule); grade 2 (mild inflammation of portal triads or lobule); grade 3 (moderate inflammation of portal triads or lobule with injury to bile duct cells); and grade 4 (severe inflammation of portal triads or lobule with necrosis and loss of bile duct cells). Acute GVHD was confirmed when the pathological grade was greater than or equal to 2.

Statistical analysis

All statistical analyses were performed using MedCalc version 15.2 (MedCalc, Mariakerke, Belgium). The normality of datasets was assessed using the Shapiro-Wilk test. The results were expressed as the median and interquartile range (IQR). Inter-observer agreement of TIC parameters was analyzed by calculating the intraclass correlation coefficient (ICC). A comparison between groups (groups at various time points; aGVHD *vs.* non- aGVHD groups) was performed using the Kruskal-Wallis H test for continuous variables. Spearman correlation analysis was used to investigate the correlations between the TIC parameters, clinical scores, serology, and pathological grade. A P value <0.05 was considered statistically significant. Logistic regression analysis was carried out to identify the TIC parameters and serologic results associated with hepatic aGVHD. Receiver operating characteristic (ROC) curve analysis based on logistic regression model for TIC parameters and serologic results and ROC curve for clinical score were performed to determine the diagnostic performance of hepatic aGVHD. The area under the

curve (AUC) was compared among the different evaluation methods using the DeLong method.

Results

Clinical manifestations of the aGVHD model

After allo-HSCT, the rats only experienced a loss of body weight during the 1st and 2nd weeks. From the 3rd week, they exhibited a hunched posture and decreased activity, ruffling of fur, maculopapular rash involving palms and soles and obvious skin exfoliation was observed in some rats until the end of the 5th week. The clinical scores of the rats continued to increase up to 5 weeks after transplantation ($P<0.05$), but there was no statistical difference for the 4th and 5th weeks compared with the 3rd week ($P>0.05$) (Figure 2A).

Histopathologic analysis

The distribution of pathological grades in each group is shown in Figure 2B. After 1w of modeling, no significant histopathological alterations were found in the rat liver. The liver of rat models exhibited mild to moderate portal vein inflammation and cholangiocellular lesions from the 2nd week. During the 3rd week, the liver pathological findings were further aggravated with loss of bile duct cells and cholestasis until the 5th week (Figure 3). The rats gradually developed aGVHD from the 2nd week with a significant increase by the 3rd week, with higher histopathological liver grades compared with the normal and 1w group ($P<0.05$), until the 5th week.

Table 1 Serological markers associated with hepatic aGVHD by univariate and multivariate regression analysis

Parameter	Univariate analysis			Multivariate analysis		
	OR	95% CI	P value	OR	95% CI	P value
ALT	1.047	0.969–1.132	0.248	1.095	0.988–1.213	0.082
AST	1.009	1.000–1.019	0.051	1.002	0.991–1.013	0.724
ALP*†	1.032	1.009–1.055	0.005	1.037	1.008–1.067	0.011

*, significant factor by univariate analysis; †, significant factor by both univariate and multivariate analyses. aGVHD, acute graft-versus-host disease; OR, odds ratio; CI, confidence interval; ALT, alanine aminotransferase; AST, aspartate aminotransferase; ALP, alkaline phosphatase.

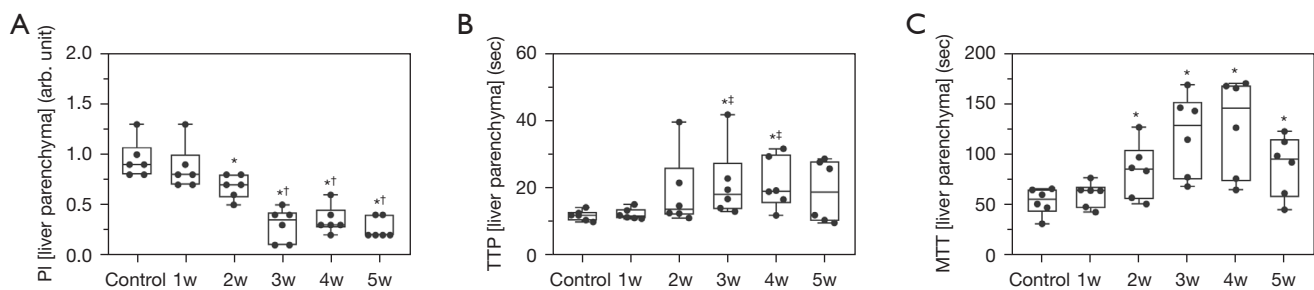


Figure 4 CEUS parameters in control group and model rats at various time points after HSCT (6 rats per group). (A) Comparison of PI across groups. (B) Comparison of TTP across groups. (C) Comparison of MTT across groups. *, $P < 0.05$ versus the control group; †, $P < 0.05$ versus the 1w group; ‡, $P < 0.05$ versus the 1w and 2w groups. w, week; CEUS, contrast-enhanced ultrasonography; HSCT, hematopoietic stem cell transplantation; PI, peak intensity; TTP, time to peak; MTT, mean transit time.

Among the 30 rats that survived allo-HSCT, 16 were diagnosed with aGVHD and the remaining rats were regarded as the non-GVHD group.

Serum test results at various time points

Figure 2C shows the serum AST, ALT and ALP values of the control and experimental groups at various time points. Compared with the normal group, the above-mentioned serum transaminase results in the late groups (especially the 4- and 5-week groups) of aGVHD were significantly elevated ($P < 0.05$). The serum AST and ALP levels in the 1- and 2-week groups exhibited no significant difference compared to normal group rats ($P > 0.05$), which increased from the third week to the end of observation in the 4- and 5-week groups. The levels of these two groups were comparable but higher than the normal, 11- and 2-week groups ($P < 0.05$). Moderate alterations in serum ALT levels were observed at various time points after modeling, and the ALT levels in the 2-, 3- and 4-week groups were higher than the normal and 1w groups ($P < 0.05$).

We further analyzed the serological markers associated with hepatic aGVHD. Univariate and multivariate regression analysis (Table 1) revealed that ALP was the only independent risk factor related to aGVHD ($P < 0.05$).

CEUS parameters analysis of hepatic aGVHD

There was excellent inter-observer consistency of CEUS parameters. The inter-observer ICC for parameters PI, TTP, MTT were 0.96 (95% CI: 0.921–0.979), 0.93 (95% CI: 0.870–0.965) and 0.89 (95% CI: 0.797–0.943), respectively.

The CEUS parameters (PI, TTP, MTT) of the normal and 1w groups were not significantly different ($P > 0.05$) (Figure 4). After HSCT, the PI gradually decreased from the second week, while MTT was significantly prolonged compared with normal group rats ($P < 0.05$). Among them, PI further decreased in the third week and remained until the fifth week ($P < 0.05$) (Figure 4A, 4C). The TTP showed a significant increase in the third week compared with the control and 1w groups ($P < 0.05$) (Figure 4B).

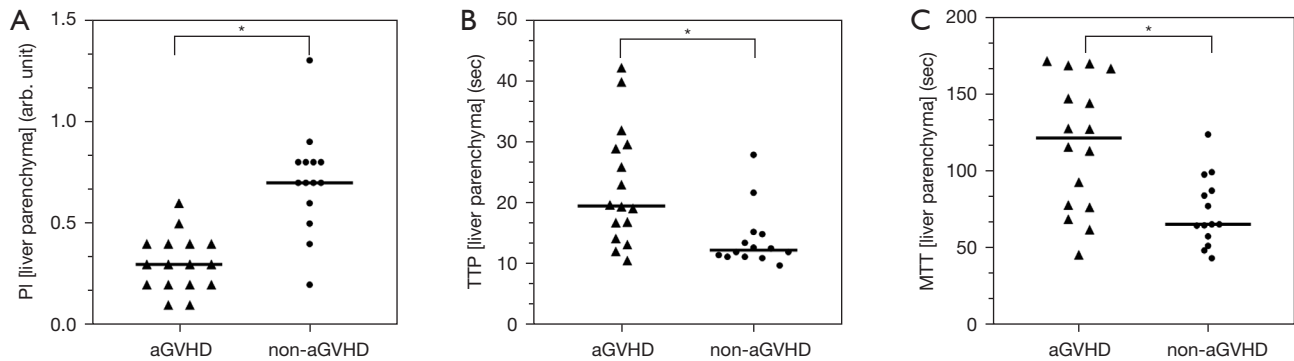


Figure 5 The CEUS quantitative parameters in acute GVHD and non-acute GVHD groups (16 and 14 rats, respectively). (A) Comparison of PI between acute GVHD and non-acute GVHD groups. (B) Comparison of TTP between acute GVHD and non-acute GVHD groups. (C) Comparison of MTT between acute GVHD and non-acute GVHD groups. *, $P < 0.05$. GVHD, graft-versus-host disease; PI, peak intensity; TTP, time to peak; MTT, mean transit time.

Table 2 CEUS parameters associated with hepatic aGVHD by univariate and multivariate regression analysis

Parameter	Univariate analysis			Multivariate analysis		
	OR	95% CI	P value	OR	95% CI	P value
PI*†	0.000	0.000–0.028	0.003	0.0001	0.000–0.144	0.014
TTP*	1.203	1.207–1.408	0.022	1.072	0.917–1.254	0.384
MTT*	1.038	1.009–1.068	0.010	1.014	0.974–1.055	0.510

*, significant factor by univariate analysis; †, significant factor by both univariate and multivariate analyses. CEUS, contrast-enhanced ultrasonography; aGVHD, acute graft-versus-host disease; OR, odds ratio; CI, confidence interval; PI, peak intensity; TTP, time to peak; MTT, mean transit time.

Figure 5 shows the CEUS quantitative parameters (PI, TTP, MTT) in aGVHD and non-aGVHD groups. The median PI of the liver in the aGVHD group was significantly lower than the non-aGVHD group [0.3 arb. unit (a.u.) (IQR, 0.2–0.4 a.u.) vs. 0.7 a.u. (IQR, 0.6–0.8 a.u.), $P < 0.05$]. The median TTP and MTT of the liver in aGVHD group were significantly higher than those in the non-aGVHD group [19.55 s (IQR, 15.5–29.25 s) and 121.5 s (77.4–156.95 s)] vs. [12.3 s (11.2–14.9 s) and 65.7 s (57.8–87.5 s)], ($P < 0.05$). These three CEUS parameters were analyzed using multivariate analysis (Table 2). Finally, PI was the only independent factor related to hepatic aGVHD ($P < 0.05$).

Correlation analysis

Table 3 presents the correlation between the CEUS parameters, clinical scores, liver enzyme levels and pathological results. CEUS parameters of hepatic

aGVHD showed a moderate to excellent correlation with pathological findings. Spearman correlation analysis revealed moderate to good positive correlations between pathological grade and the parameters TTP and MTT. In contrast, an excellent negative correlation was found between PI and pathological grade, which was higher than the correlation between pathological findings and the clinical score and serological markers.

Diagnostic performance of various approaches in detecting hepatic aGVHD

The AUC of CEUS parameter, clinical score, and serology for the diagnosis of hepatic aGVHD were 0.933 (95% CI: 0.779–0.992), 0.748 (95% CI: 0.557–0.888) and 0.902 (95% CI: 0.737–0.980), respectively (Figure 6). The AUC of CEUS parameters was significantly greater than that of clinical scores ($P = 0.032$) but comparable to the serological results ($P = 0.694$).

Table 3 Correlation between pathological grade and CEUS parameters, clinical score, and serology

Pathology	Clinical score	Serological markers			CEUS		
		ALT	AST	ALP	PI	TTP	MTT
r	0.699	0.526	0.526	0.685	-0.843	0.581	0.601
P	<0.001	0.001	0.001	<0.001	<0.001	<0.001	0.001

CEUS, contrast-enhanced ultrasonography; ALT, alanine aminotransferase; AST, aspartate aminotransferase; ALP, alkaline phosphatase; PI, peak intensity; TTP, time to peak; MTT, mean transit time.

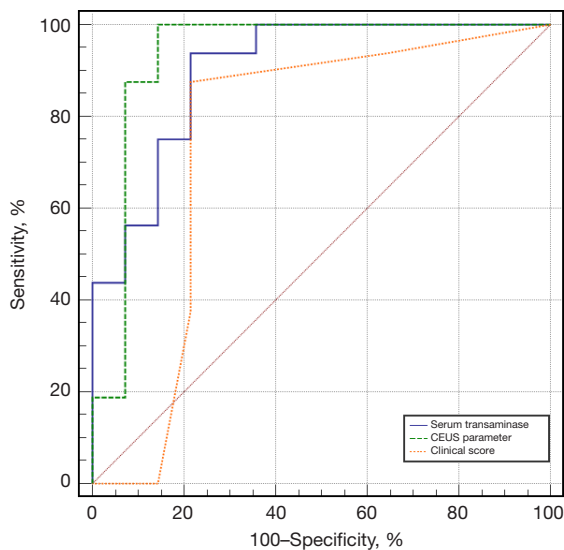


Figure 6 ROC curve of CEUS parameter, clinical score, and serology for detecting hepatic acute GVHD. ROC, receiver operating characteristic; CEUS, contrast-enhanced ultrasonography; GVHD, graft-versus-host disease.

Discussion

GVHD has been suggested to be a major complication with high morbidity and mortality after allo-HSCT, its diagnosis primarily relies on clinical and laboratory findings, but currently there is lack of an effective non-invasive imaging tool for the early diagnosis and surveillance of GVHD. CEUS is a real-time angiographic imaging technique used to visualize microcirculation to fully understand the organ function, which can be performed at the bedside, especially for severely ill patients. The present study investigated the clinical characteristics, serum enzyme levels, histopathological features and CEUS quantitative parameters of rats after HSCT, indicating that the diagnostic value of CEUS for hepatic aGVHD was superior to clinical scores and serology.

We found a significant increase in serum AST and ALP levels in rats during the third week and ALT levels during the second week after HSCT compared with the normal group ($P < 0.05$), which may be caused by cholestatic liver derangement after transplantation (23,24). Among them, the ALP level was significantly increased compared to transaminases, consistent with the literature (25). In this regard, serum ALP level has been described as a sensitive diagnostic marker for liver GVHD, similar to serum bilirubin levels (26). At the same time, we found that rats with abnormal liver enzyme levels also had evidence of histopathological liver damage. During the second week after modeling, we observed mild to moderate portal vein inflammation and cholangiocellular lesions in the liver, and the lesions exacerbated over time, accounting for higher pathological grades in the 4w and 5w groups ($P < 0.05$). Multivariate regression analysis showed that ALP was the only predictor of hepatic aGVHD. In recent years, studies have emphasized the role of liver enzymes in the diagnosis of hepatic GVHD and considered it an important part of the diagnostic criteria (25-27). However, it should be borne in mind that liver enzyme levels are not always perfectly correlated with liver histological changes (28). Accordingly, a liver biopsy is indicated for a definite diagnosis to rule out other causes for suspected hepatic GVHD based on clinical data. Liver biopsy is an invasive procedure with a 1.3–20.2% complication rate for transjugular liver biopsy (27) but not indicated for frequent follow-up examinations. Based on our current knowledge of GVHD, we explored the value of CEUS in acute hepatic GVHD, which may be of great clinical utility.

PI began to decrease in the second week after HSCT, earlier than ALP, which could accurately reflect the histopathological changes and detect liver damage at an early stage. Moreover, the TIC parameters of aGVHD group, including PI, TTP and MTT, were significantly different from those of the non-aGVHD group ($P < 0.05$). Compared with the non-aGVHD group, the PI was

lower in the aGVHD group, while TTP and MTT were higher. This trend in CEUS parameters suggested that hepatic blood perfusion was reduced, and microcirculation dysfunctions occurred. An increasing body of evidence suggests that acute hepatic GVHD commonly presents as a cholestatic pattern of liver injury, and histological findings include cholangitis, bile-duct destruction, and lymphocytic infiltration of the portal areas (6,22,29). Although the hepatocellular damage is mild, these above histological changes may affect the liver hemodynamics, limiting the full filling of veins and resulting in a decrease in the volume of portal vein and blood flow velocity, thereby reducing hepatic parenchyma perfusion and prolonging perfusion time. Current evidence suggests that progressive liver fibrosis may occur if GVHD persists (30), suggesting that CEUS may play a role in the early stages of liver disease. Thus, in clinical practice, when there is no increase in serum markers and no positive findings on conventional ultrasound (including color Doppler ultrasound) of patients after transplantation in early stage, CEUS of the liver can be performed in post-transplant patients with high-risk factors for aGVHD (such as HLA mismatch, receipt of a transplant from an unrelated donor, a female donor for a male recipient, and so on) or with other target organs involvement (such as skin and gastrointestinal tract) to diagnose early and obtain the optimal therapeutic efficacy. However, it cannot be used in patients with allergic to ultrasound contrast agents, or in patients with recent acute coronary syndrome or clinically unstable ischemic heart disease. In this case, shear-wave elastography can be performed to describe the mechanical properties of the tissue and further assess liver injury based on color Doppler ultrasound results, as it has been suggested to effectively predict liver events and total mortality in the early period and the first year after allo-HSCT.

Regarding clinical presentation, rats exhibited only weight loss within the first two weeks after modeling. Interestingly, ruffling of fur and a maculopapular rash appeared from the third week. The weight loss in the previous two weeks may be partly due to radiation-induced immunosuppression and poor appetite in rats before modeling. Even though rats are quite sensitive to radiation, especially the liver, the damage is often reversible (31). Thus, the clinical symptoms were further aggravated after the onset of aGVHD. In our study, CEUS yielded better diagnostic performance in detecting hepatic aGVHD than clinical scores, while was comparable to serology. However, the correlation between CEUS parameters and

histopathology was higher than that of serology, suggesting that CEUS may be superior to serology for the early diagnosis and assessment of the severity of GVHD.

There remain several limitations in this study. First, our sample size was small, and the number of rats for each pathological grade was limited. Only 2 rats were included in grade 2, which may have reduced the statistical power of CEUS for different grades of hepatic aGVHD, although our primary goal was achieved. Besides, compared with CT and MR, CEUS is an operator-dependent examination with more subjectivity. However, we analyzed the TIC curves to obtain quantitative parameters using data processing software to minimize deviations. Moreover, the inter-operator consistency test confirmed the reliability of the data. In addition, we did not study the value of CEUS in differentiating from other hepatic complications secondary to allo-HSCT, including venoocclusive disease and cytomegalovirus hepatitis (32), which can guide clinicians during treatment and management. These issues should be fully addressed in future studies to ensure that findings from animal experiments can be translated into clinical practice.

Conclusions

CEUS can be used to monitor the microcirculation dysfunction of hepatic aGVHD after allo-HSCT, which reflects histopathological changes in the liver. CEUS has an exciting prospect for clinical application in identifying GVHD and early liver damage by analyzing TIC curves to obtain quantitative parameters.

Acknowledgments

We thank the editorial team with Home for Researchers (www.home-for-researchers.com) for language editing service.

Funding: This study was supported by the National Natural Science Foundation of China (No. 82001826 to Yiqun Liu).

Footnote

Reporting Checklist: The authors have completed the ARRIVE reporting checklist. Available at <https://qims.amegroups.com/article/view/10.21037/qims-22-1145/rc>

Conflicts of Interest: All authors have completed the ICMJE uniform disclosure form (available at <https://qims.amegroups.com/article/view/10.21037/qims-22-1145/coif>).

The authors have no conflicts of interest to declare.

Ethical Statement: The authors are accountable for all aspects of the work in ensuring that questions related to the accuracy or integrity of any part of the work are appropriately investigated and resolved. The study was approved by the Animal Care and Use Committee of Peking University People's Hospital (License number: 2020PHE088). All experimental procedures were performed according to the Guide for the Care and Use of Laboratory Animals.

Open Access Statement: This is an Open Access article distributed in accordance with the Creative Commons Attribution-NonCommercial-NoDerivs 4.0 International License (CC BY-NC-ND 4.0), which permits the non-commercial replication and distribution of the article with the strict proviso that no changes or edits are made and the original work is properly cited (including links to both the formal publication through the relevant DOI and the license). See: <https://creativecommons.org/licenses/by-nc-nd/4.0/>.

References

1. Sacirbegovic F, Günther M, Greco A, Zhao D, Wang X, Zhou M, Rosenberger S, Oberbarnscheidt MH, Held W, McNiff J, Jain D, Höfer T, Shlomchik WD. Graft-versus-host disease is locally maintained in target tissues by resident progenitor-like T cells. *Immunity* 2023;56:369-385.e6.
2. Cooper JP, Abkowitz JL. How I diagnose and treat acute graft-versus-host disease after solid organ transplantation. *Blood* 2023;141:1136-46.
3. Zeiser R, Teshima T. Nonclassical manifestations of acute GVHD. *Blood* 2021;138:2165-72.
4. Pasquini MC, Wang Z. Current Use and Outcome of Hematopoietic Stem Cell Transplantation: Part I—Cibmtr Summary Slides. *CIBMTR Newsletter [Serial Online]* 2007;15:7-11.
5. Arai Y, Kanda J, Nakasone H, Kondo T, Uchida N, Fukuda T, Ohashi K, Kaida K, Iwato K, Eto T, Kanda Y, Nakamae H, Nagamura-Inoue T, Morishima Y, Hirokawa M, Atsuta Y, Murata M; . Risk factors and prognosis of hepatic acute GvHD after allogeneic hematopoietic cell transplantation. *Bone Marrow Transplant* 2016;51:96-102.
6. Modi D, Ye JC, Surapaneni M, Singh V, Chen W, Jang H, Deol A, Ayash L, Alavi A, Ratanatharathorn V, Uberti JP. Liver Graft-Versus-Host Disease is associated with poor survival among allogeneic hematopoietic stem cell transplant recipients. *Am J Hematol* 2019;94:1072-80.
7. Mahgerefteh SY, Sosna J, Bogot N, Shapira MY, Pappo O, Bloom AI. Radiologic imaging and intervention for gastrointestinal and hepatic complications of hematopoietic stem cell transplantation. *Radiology* 2011;258:660-71.
8. Zeiser R, Blazar BR. Acute Graft-versus-Host Disease - Biologic Process, Prevention, and Therapy. *N Engl J Med* 2017;377:2167-79.
9. Zhang M, Mendiratta-Lala M, Maturen KE, Wasnik AP, Wang SS, Assad H, Rubin JM. Quantitative Assessment of Liver Stiffness Using Ultrasound Shear Wave Elastography in Patients With Chronic Graft-Versus-Host Disease After Allogeneic Hematopoietic Stem Cell Transplantation: A Pilot Study. *J Ultrasound Med* 2019;38:455-61.
10. Ferrara JL, Levine JE, Reddy P, Holler E. Graft-versus-host disease. *Lancet* 2009;373:1550-61.
11. Shulman HM, Cardona DM, Greenson JK, Hingorani S, Horn T, Huber E, et al. NIH Consensus development project on criteria for clinical trials in chronic graft-versus-host disease: II. The 2014 Pathology Working Group Report. *Biol Blood Marrow Transplant* 2015;21:589-603.
12. Zhou H, Zhang C, Du L, Jiang J, Zhao Q, Sun J, Li Q, Wan M, Wang X, Hou X, Wen Q, Liu Y, Zhou X, Huang P. Contrast-Enhanced Ultrasound Liver Imaging Reporting and Data System in Diagnosing Hepatocellular Carcinoma: Diagnostic Performance and Interobserver Agreement. *Ultraschall Med* 2022;43:64-71.
13. Kayali S, Pasta A, Pellicano R, Fagoonee S, Giuliana E, Facchini C, Pili S, Buccilli S, Labanca S, Borro P. Effect of contrast-enhanced ultrasound (CEUS) on liver stiffness measurements obtained by transient and shear-wave elastography. *Panminerva Med* 2022;64:479-84.
14. Weber D, Weber M, Hippe K, Ghimire S, Wolff D, Hahn J, Evert M, Herr W, Holler E, Jung EM. Non-invasive diagnosis of acute intestinal graft-versus-host disease by a new scoring system using ultrasound morphology, compound elastography, and contrast-enhanced ultrasound. *Bone Marrow Transplant* 2019;54:1038-48.
15. Pausch AM, Kammerer S, Weber F, Herr W, Stroszczyński C, Holler E, Edinger M, Wolff D, Weber D, Jung EM, Wertheimer T. Parametric Imaging of Contrast-Enhanced Ultrasound (CEUS) for the Evaluation of Acute Gastrointestinal Graft-Versus-Host Disease. *Cells* 2021.
16. Tian Y, Deng YB, Huang YJ, Wang Y. Bone marrow-derived mesenchymal stem cells decrease acute graft-versus-host disease after allogeneic hematopoietic stem cells transplantation. *Immunol Invest* 2008;37:29-42.

17. Ryu H, Kim JH, Lee S, Han JK. Therapeutic response monitoring after targeted therapy in an orthotopic rat model of hepatocellular carcinoma using contrast-enhanced ultrasound: Focusing on inter-scanner, and inter-operator reproducibility. *PLoS One* 2020;15:e0244304.
18. Wang Y, Xie X, Cao Q, Xie W, Chen D, Zhang X, Guo Y, Zhou L. Quantitative Contrast-Enhanced Ultrasound by Sonazoid in the Early Diagnosis of Biliary Atresia: An Experimental Study of Rats With Bile Duct Ligation. *Ultrasound Med Biol* 2019;45:2767-76.
19. Cooke KR, Kobzik L, Martin TR, Brewer J, Delmonte J Jr, Crawford JM, Ferrara JL. An experimental model of idiopathic pneumonia syndrome after bone marrow transplantation: I. The roles of minor H antigens and endotoxin. *Blood* 1996;88:3230-9.
20. Dietrich CF, Nolsøe CP, Barr RG, Berzigotti A, Burns PN, Cantisani V, et al. Guidelines and Good Clinical Practice Recommendations for Contrast-Enhanced Ultrasound (CEUS) in the Liver-Update 2020 WFUMB in Cooperation with EFSUMB, AFSUMB, AIUM, and FLAUS. *Ultrasound Med Biol* 2020;46:2579-604.
21. Liu F, Li D, Xin Y, Liu F, Li W, Zhu J. Quantification of Nerve Viscosity Using Shear Wave Dispersion Imaging in Diabetic Rats: A Novel Technique for Evaluating Diabetic Neuropathy. *Korean J Radiol* 2022;23:237-45.
22. Blatter DD, Crawford JM, Ferrara JL. Nuclear magnetic resonance of hepatic graft-versus-host disease in mice. *Transplantation* 1990;50:1011-8.
23. Hatami B, Mosala M, Hassani AH, Ardakani MJE, Gholami S, Zali MR. Fenofibrate in primary sclerosing cholangitis; a randomized, double-blind, placebo-controlled trial. *Pharmacol Res Perspect* 2022;10:e00984.
24. Yang Y, Chen Y, Zhao Y, Ji F, Zhang L, Tang S, Zhang S, Hu Q, Li Z, Zhang F, Li Q, Li L. Human menstrual blood-derived stem cell transplantation suppresses liver injury in DDC-induced chronic cholestasis. *Stem Cell Res Ther* 2022;13:57.
25. Hockenbery DM, Strasser SI, McDonald GB. Gastrointestinal and hepatic complications. In: Forman SJ, Negrin RS, Antin JH, et al. (editors). *Thomas' hematopoietic cell transplantation*. 5th ed. Hoboken: Wiley, 2016.
26. Ashizawa M, Oshima K, Wada H, Ishihara Y, Kawamura K, Sakamoto K, Sato M, Terasako K, Machishima T, Kimura S, Kikuchi M, Nakasone H, Okuda S, Kako S, Kanda J, Yamazaki R, Tanihara A, Nishida J, Kanda Y. Hyperbilirubinemia in the early phase after allogeneic HSCT: prognostic significance of the alkaline phosphatase/total bilirubin ratio. *Bone Marrow Transplant* 2013;48:94-8.
27. Ma SY, Au WY, Ng IO, Lie AK, Leung AY, Liang R, Lau GK, Kwong YL. Hepatic graft-versus-host disease after hematopoietic stem cell transplantation: clinicopathologic features and prognostic implication. *Transplantation* 2004;77:1252-9.
28. Akpek G, Boitnott JK, Lee LA, Hallick JP, Torbenson M, Jacobsohn DA, Arai S, Anders V, Vogelsang GB. Hepatic variant of graft-versus-host disease after donor lymphocyte infusion. *Blood* 2002;100:3903-7.
29. Fujii N, Takenaka K, Shinagawa K, Ikeda K, Maeda Y, Sunami K, Hiramatsu Y, Matsuo K, Ishimaru F, Niiya K, Yoshino T, Hirabayashi N, Harada M. Hepatic graft-versus-host disease presenting as an acute hepatitis after allogeneic peripheral blood stem cell transplantation. *Bone Marrow Transplant* 2001;27:1007-10.
30. Le Floc'h A, Nagashima K, Birchard D, Scott G, Ben LH, Ajithdoss D, et al. Blocking common γ chain cytokine signaling ameliorates T cell-mediated pathogenesis in disease models. *Sci Transl Med* 2023;15:eabo0205.
31. Feng J, Chen SB, Wu SJ, Sun P, Xin TY, Chen YZ. Quantitative analysis of contrast-enhanced ultrasonography in acute radiation-induced liver injury: An animal model. *Exp Ther Med* 2015;10:1807-11.
32. Trenker C, Burchert A, Schumacher C, Schäfer JA, Dohse M, Timmesfeld N, Neubauer A, Sohlbach K, Michel C, Görg C. Pathologic Hepatic Contrast-Enhanced Ultrasound Pattern in Patients Undergoing Allogeneic Stem Cell Transplantation. *Ultrasound Med Biol* 2020;46:1865-71.

Cite this article as: Xin Y, Xiong Y, Liu F, Qu L, Li W, Yang L, Liu Y, Zhu J. Quantitative analysis of contrast-enhanced ultrasonography in rat models of hepatic acute graft-versus-host disease. *Quant Imaging Med Surg* 2023;13(8):4908-4918. doi: 10.21037/qims-22-1145